Received: 8 December 2020 | Accepted: 9 December 2021

DOI: 10.1002/vzj2.20184

Vadose Zone Journal

TECHNICAL NOTES

A device to simulate contaminant transfer and surface and subsurface flow through intact soil monoliths

Nico Hachgenei[1] | **Guillaume Nord**[1] | **Lorenzo Spadini**[1] | **Henri Mora**[1] | **François Courvoisier**[1] | **Jean-François Sutra**[2] | **Jean-Pierre Vandervaere**[1] | **Cédric Legoût**[1] | **Marie-Christine Morel**[1,3] | **Jean Martins**[1] | **Anne Lespine**[2] | **Celine Duwig**[1]

[1]IGE, Univ. Grenoble Alpes, CNRS, IRD, Grenoble INP, Grenoble 38000, France

[2]INTHERES, INRAE, ENVT, Univ. de Toulouse, Cedex 3, Toulouse 31076, France

[3]le CNAM, Laboratoire d'analyses chimiques et bio analyses, Cedex 3, Paris, France

Correspondence
Céline Duwig, IGE, CNRS, IRD, Univ. Grenoble Alpes, Grenoble INP, Grenoble, 38000, France.
Email: celine.duwig@ird.fr

Assigned to Associate Editor Vilim Filipović.

Funding information
Agence Nationale de la Recherche, Grant/Award Number: #ANR-10-LABX-56; Institut National des Sciences de l'Univers, Centre National de la Recherche Scientifique, Grant/Award Numbers: SNO SIC ANO-1, Zone critique et eau continentale/OHMCV

Abstract

Many contaminants of agricultural origin are released into rural environments, particularly at the soil surface. Their fate has been extensively investigated in repacked soils, but only few studies have addressed their transport in structurally preserved natural soils. Much remains unknown about their fate and transfer within and between environmental compartments, while the susceptibility of these compartments to the contaminants adverse effects can vary considerably. The lack of studies regarding surface and subsurface transfer of contaminants through intact soil compared with studies on repacked soil led us to propose a device and protocol for sampling intact soil monoliths (60 × 30 × 22 cm^3, length, width, depth [LWD]) without heavy machinery. This is achieved by a modular design with removable top and bottom lid and a protocol of cutting the soil and replacing the affected bottom soil with a drainage layer of glass beads. The device allows the application of artificial rainfall events with simultaneous highly resolved quantification of infiltration excess overland flow and drainage discharge. It is designed to facilitate the collection of samples for physical, biological, and chemical analyses that fulfill cleanliness standards for organic contaminant analysis at trace levels using only poorly reactive stainless steel and glass materials. Testing of the device was performed by measuring the transfer of the antiparasitic drug ivermectin (IVM) through and over a silt-loam pasture soil. This test case illustrates how the device can be used to gain valuable information on the transfer of trace organic contaminants through topsoils.

Abbreviations: CR, overland flow coefficient; D_m, mean diameter; IVM, ivermectin/22,23-Dihydroavermectin B_1; LWD, length, width, depth; PI, precipitation intensity; Q_D, drainage discharge; Q_R, overland flow discharge.

1 | INTRODUCTION

Soils are exposed to a large number of contaminants of different types (e.g., pharmaceuticals [Obimakinde et al., 2017], pesticides [Hedlund et al., 2020], pathogenic bacteria [Bicudo & Goyal, 2003; Chen et al., 2021] and microplastics [Nizzetto et al., 2016]). These compounds are often applied directly or indirectly to soil surfaces in a variety of ways. From there, they can be transported to other environmental compartments. Some of these contaminants have adverse effects on different environmental compartments such as soil, surface water, and groundwater (Boxall, 2017; Schäfer et al., 2007). The environmental risk of a compound can be evaluated by comparing predicted no-effect concentrations to predicted environmental concentrations (e.g., Liebig et al., 2010; Stuer-Lauridsen et al., 2000). The latter are often obtained via numerical modeling, using simplified assumptions for water flow.

Various studies emphasize the importance of soil structure, which determines the configuration of the soil pore system and thereby controls movement of water and contaminants through soil as well as surface–subsurface flow repartition (Bachmair et al., 2009; Chen et al., 2021; Duwig et al., 2019; Flury et al., 1994; Martín et al., 2017). Flury et al. (1994) studied flow patterns in 14 soils, in the field and concluded that bypass flow is stronger in structured soils, which therefore present an elevated risk for contaminant leaching. Bachmair et al. (2009) studied vertical and horizontal patterns of water infiltration into five different soils and identified different soil features being responsible for the observed patterns in the different soils, including the pore structure, surface microtopography, surface cover, water repellency as well as topsoil matrix characteristics such as bulk density and organic matter content. Natural root systems, micro and macrofauna as well as drying cracks in clayey soils greatly affect the soil porous system (Milleret et al., 2009). The soil surface structure (microtopography and crusts) also essentially affects flow repartition between surface and subsurface (Carmi & Berliner, 2008; Govers et al., 2000). Furthermore, surface microtopography may affect the contact surface and contact time between soil and water as it determines hydraulic roughness and more or less concentrated overland flow paths (Darboux et al., 2002; Govers et al., 2000; Hairsine et al., 1992). Repacked soil does not mimic the internal and surface structure of natural soil and therefore fails to reproduce natural flow patterns that would occur in situ (Boyle et al., 1989; Franzluebbers, 2002). Repacked soil favors matrix flow compared with preferential flow (Guo & Chorover, 2006) leading to reduced contaminant transfer and decreased saturated hydraulic conductivity (Chen et al., 2021; Sadeghi et al., 2000). This generally hinders infiltration and increases overland flow, which is known to be an important vector of contaminants (Sarmah et al., 2006). The difference between repacked and intact soil is expected to be particularly effective for intense storm events that result in a high proportion of rapid preferential flow and overland flow. Therefore, in order to better evaluate the risk of contaminant transfer through and over soils, it seems crucial to study transfer through and over intact soil that includes native vegetation with well-developed root channels, biopores, and other features of the natural soil structure as described above.

Core Ideas

- A device for collecting intact soil and subjecting it to artificial rainfall was developed.
- The setup allows for high resolution measurement and sampling of drainage and overland flow.
- It is designed for clean sampling permitting analysis of various contaminants at trace levels.
- We present an experiment to test the device on transfer of ivermectin from cow dung.

Different techniques for the sampling of intact soil exist. Sampling techniques can be coarsely classified into two categories, either a sampling frame is forced into the soil (Feyereisen & Folmar, 2009), or the surrounding soil is removed and the soil sample is then surrounded by a support structure and the sides are sealed with substances like concrete or resins (Benecke et al., 1976; Buchter et al., 1984; Krogmann, 1986). The first one has the advantage of being relatively simple, but is not adapted for soils containing stones, as forcing on these stones destroys the structure of the soil. Furthermore, this technique depends on heavy machinery in order to push the frame into the soil and is therefore limited to well accessible sampling locations. The second technique is more adapted for a large variety of soils; however, the use of resin or concrete should be avoided in experiments on the transfer of organic contaminants at trace levels. These compounds require the use of inert material that does not interact with the studied compounds and allows cleaning with organic solvents or heat treatment of the parts that are reused.

There are different approaches to studying contaminant transfer through soils using dynamic experiments under controlled conditions. Three types of approaches have been commonly used in other studies: (a) Soil columns (Archundia et al., 2019; Kay et al., 2005b; Rath et al., 2016) are often small and inexpensive, allowing the study of basic chemical and physical processes underlying contaminant transfer through the soil matrix under controlled conditions and generating reproducible results. However, the applicability of their results to environmental systems is limited because they do not account for some important soil properties and processes: structure (soils are often repacked), vegetation cover, overland flow, erosion and transport of particles. (b) Lysimeters (Goss

et al., 2010; Kay et al., 2005a) are an excellent tool for in-situ studies of long-term vertical transfer through intact soil and the potential for leaching of contaminants into groundwater. However, they are often complex and expensive pieces of equipment and installations, making them less convenient for testing specific factors on multiple soils and for investigations on the scale of a few simulated intense rainfall events. Furthermore, they are often not designed for quantification and sampling of overland flow. (c) 2D-Soil boxes have been used by some authors to study the transfer of pharmaceuticals, by drainage and overland flow (Fernández et al., 2011; Popova et al., 2013). However, the only well documented design allowing the use of intact soil for surface and subsurface transfer studies of organic contaminants that the authors could find uses heavy machinery to push the sampling frame into the soil (Feyereisen & Folmar, 2009). This restricts them to accessible sampling locations and stone-free soils. Therefore, we state the need of an experimental device and protocol to study pollutant transfer through and over a wide range of intact soils under simulated rainfall in controlled conditions. This device should allow to test the effect of different factors such as rainfall intensity, initial soil moisture, slope and soil type on the transfer of contaminants, while using all stainless-steel equipment and capturing the intra-event dynamics of water and pollutant fluxes at a high temporal resolution.

We developed a hand maneuverable system that allows to sample a 60 × 30 × 22 cm^3 (length, width, depth [LWD]) intact soil cuboid in the field. The sampling device fits in a rainfall simulator and allows high-frequency measurement and sampling of drainage and overland flow. The system is entirely designed in stainless steel, to minimize chemical interactions with the studied organic molecules. The use of intact soil allows for a realistic soil response and the ex-situ rainfall simulation allows for controlled conditions and monitoring of all fluxes while avoiding contaminating the study site. This device can provide insight into the hydrological behavior of natural topsoils under different conditions and forcing as well as the transfer of different types of contaminants (trace organic molecules such as pharmaceuticals and pesticides, bacteria and viruses, particles such as microplastics, metallic trace elements).

This paper presents the sampling strategy, the experimental setup, the limitations of the system, and potential applications. A technical validation experiment was conducted by studying the transfer of ivermectin (IVM), a common livestock antiparasitic drug, from artificially contaminated cow dung on an agricultural soil.

2 | MATERIALS AND METHODS

2.1 | General design of the experimental device

2.1.1 | The rainfall simulator

The rainfall simulator consists of a support for the soil box, a rainfall simulator frame for the sprinkler, a booster (pump with pressurized water reservoir), one or several water reservoirs, a rain collector frame surrounding the upper edge of the soil box and a transparent PVC chimney (Figure 1). The soil box support has an adjustable slope (0–18° [0–32.7%], 8° in this work). The height-adjustable aluminum rainfall simulator frame (total height 114 cm) accommodates a sprinkler nozzle, a battery or mains operated motor that rotates the nozzle continuously at 65 rpm, a pressure gauge, and spigots. We have tested different full cone sprinkler nozzles of the Lechler 490 series generating intensities ranging from 50 mm h^{-1} (490.488.30) to 100 mm h^{-1} (490.608.30). The nozzles are easily exchangeable to adjust the rainfall intensity. They generally generate fine drops with little kinetic energy. This choice of finer raindrops was made in order to better preserve the soil structure from one experiment to the next. This allows comparing the soils reaction in different conditions (e.g., wet vs. dry) on a soil that had been formed by natural rainfall in the field although it limits soil erosion that would be expected with such intense precipitation (see Discussion section for more detail).

The booster (Mac Allister 900W) generates a pressure fluctuating between 1.4 and 2.8 bar. It is connected to a pressure regulator to minimize variations in output pressure. The booster is fed by 100-L water reservoirs, in which water tracers can be applied. The rain collector frame covers 1.5 cm of the soil's edges and collects all the rainwater falling onto these edges and outside the soil surface by means of the PVC chimney. The excess rainwater is returned to the reservoir. During the rainfall simulation, a short PVC hose is connected to each of the two outlets of the soil box (drainage and overland flow) to conduct the flow to glass containers placed on scales. In our test, we used a Denver Instrument S-2002 (2 kg max, d = 0.01 g) for overland flow and a Precia Molen X201-B (30 kg max, d = 1 g) for drainage. The scales are connected to a PC that records mass values at 1 Hz. There are no depressions in the flow path between soil and sample collection that could accumulate water and hinder flow continuity. This ensures the samples to contain both the liquid fraction and the suspended matter.

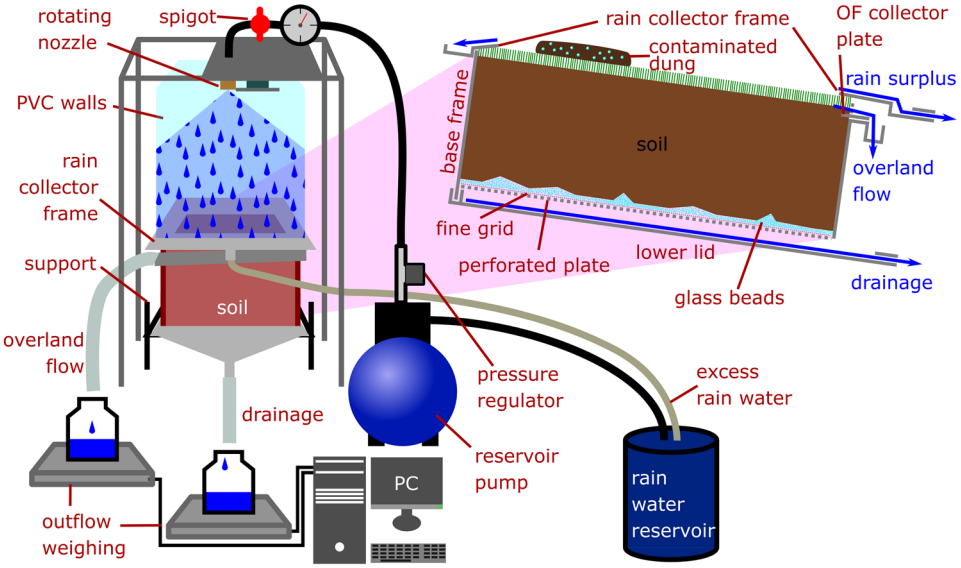

FIGURE 1 Schematic illustration of the rainfall simulation setup and a 2D longitudinal cut through the sampling box

2.1.2 | The sampling box

The sampling box is illustrated in Figure 1. It is made entirely of stainless steel in order to minimize chemical interactions with the studied organic molecules and allow cleaning with an organic solvent (acetonitrile) or thermal treatment. Blueprints and photos are provided in Supplemental Figures S1–S3. It consists of a $60 \times 30 \times 25$ cm^3 (LWD) base frame and removable bottom and top lids. The base frame includes a horizontally mounted removable 0.7-mm wire grid with 2-mm gaps, supported by a 3-mm thick perforated plate with 5-mm square holes, mounted 22 cm from the top of the frame. The perforated plate is supported by a mount welded to the bottom lid. On the downhill side, the top 3 cm of the base frame is perforated with 5-mm square holes to allow overland flow to pass through. A gap below the perforated portion allows for the insertion of a $3 \times 296 \times 90$ mm^3 overland flow collector plate into the soil 3 cm from the surface of the box. An inclined U-shaped profile with an outlet (2-cm pipe) on the side is welded to this side of the base frame allowing for the collection of overland flow. The bottom lid is designed to collect the drainage flow. Its downhill end converges to a 2-cm pipe for water collection. The top lid is only used during soil sampling. Both lids are attached to the base frame with stainless steel toggle latches (RS PRO).

2.2 | Procedure for sampling intact soil in the field

The soil sampling protocol is designed to preserve the soil structure. Sampling should be done under intermediate to dry conditions, in order to avoid sampling very soft to liquid muddy soil, which would lose its structure. Under very dry conditions, the soil should be slightly moistened with purified water to soften it and ensure sufficient cohesion during cutting. The required water content depends on the soil type. In practice, gradual moistening of an area close to the sampling location can help determine the right amount of moistening that provides cohesion without making the soil muddy. The soil sample should be selected in a representative location (vegetation, land use, slope, part of the hillslope). The original slope should correspond approximately to the slope that will be used in the experiment. The sample should have a relatively even surface. The following sampling procedure is divided into 12 numbered steps, a selection of which is shown in Supplemental Figure S4. The positional terms used are depicted in Supplemental Figure S1. (1) The sampling frame is placed at the selected sampling location, oriented with the outlet pointing down the slope. (2) A trench approximately 35-to-40-cm deep, 1.5-m long and 1-m wide is excavated on one side of the selected sample location for easy access to the soil from the side. A narrower trench is dug on the other three sides while leaving 5–10 cm of intact soil on each side of the sample to protect it.

The frame is gradually lowered around the sample by repeating the following four steps (3–6) a few centimeters each time until the soil surface is aligned with the top edge of the sampling case (not extending beyond the frame's upper edge and not being more than 15 mm below it): (3) The soil is carefully cut to fit the case. (4) Small rocks protruding from the side are removed and the holes are filled with wet, compacted original soil. If a hole is too large (more than a few centimeters of diameter), changing the sampling location should be considered. (5) The sidewalls are covered with bentonite clay to seal them before (6) sliding the case along the walls

(perpendicularly to the soil surface). (7) The cutting of the bottom of the soil starts by making a set of horizontal bores below the bottom of the soil from the side using a battery powered drill with a rock drill bit. Then (8) 6 mm (35-mm wide) steel blades are carefully hammered into the bores, one by one, next to each other, from the side, to support the soil. (9) The top of the soil sample is covered with a lid attached to the base frame. Two steel bars are slid under the blades in longitudinal orientation (perpendicularly to the blades). Two other steel bars are placed on top of the sample and screwed to the bottom bars with four 32-cm long M10 threaded rods. This step serves to firmly hold the sample. (10) The sample is lifted by hand (three people) and turned upside down by slowly rolling it over the edge of the hole. With the sample held firmly in the frame, disturbance should be minimal when turning the sample slowly. After removing the steel bars, (11) the bottom 3 cm of soil that was potentially affected by the steel blades is removed. To ensure a uniform surface of the bottom of the soil and to distribute the soil's weight, (12) a thin layer (<1 cm) of 4-mm glass spheres is added before closing with the grid, the perforated plate and the lid firmly clipped onto the bottom soil. The sample is then turned upright for transport to the laboratory. Prior to the rainfall simulation experiments, the overland flow collector plate is entered horizontally into the upper soil on the downhill side of the box (1-cm deep, 3 cm below the frames upper edge; see Figure 1). Finally, the upper edges of the soil are sealed with a mixture of field soil matrix and water. This sealing as well as the rain collector frame covering the boundaries are used to prevent infiltration through potential gaps along the sidewalls. We could not apply petroleum jelly as used by other authors (e.g., Williams et al., 2020) because of potential chemical interferences with the studied contaminants. However, in addition to the measures described above, flow along gaps between the sidewalls and the soil should be limited as long as the soil is in unsaturated condition. Vegetation is cut to a level below the rain collector frame.

2.3 | Rainfall simulation experiment

2.3.1 | Measured variables

Artificial rainfall is applied at the selected intensity and duration. In the test case section, we present two nozzles that allow to obtain intensities of 50 and 100 mm h^{-1}. Drainage and overland flow are collected in separate, pre-weighed sample containers placed on two scales. The mass values are transmitted to a PC via a serial port at 1 Hz and stored together with the time in a ".csv" file. Because of the flow monitoring via mass values, special care must be taken when changing the sampling containers: First, the hose is moved to the new container. After waiting 3 s, the old container is removed and the new one is placed on the scale. The times of moving the hose and placing the new container are noted, as well as the ID of each pre-weighed container. The mass values during the container change are removed from the mass time series. The soil is weighed with the box before and after the rainfall simulation experiment. The difference gives the change in soil water storage (ΔS_{TOT}).

2.3.2 | Calculated variables

The mass values of the empty containers are systematically subtracted from the mass time series and after each container change, the previous mass is added to all subsequent timesteps by a python program. This provides a cumulative time series for each water outflow (drainage and overland flow), assuming that all mass recovered is water and has a density of 1 g ml^{-1}. The water volume can be converted to water height by dividing it by the soil surface (30×60 cm^2). The values at the last timestep of these series are the total outflow volume of the drainage (VD_{TOT}) and overland flow (VR_{TOT}). The instantaneous water discharges of drainage $Q_D(t)$ and overland flow $Q_R(t)$ at each time t are obtained by dividing the volume difference by time difference between two consecutive measurements. Weighing is continued for several hours after the end of rain application (until dripping stops) to capture all outflow water.

The total soil water content at the beginning (V_{sw0}) and end (V_{swf}) of each experiment is obtained by subtracting the weight of the whole soil dried at 105 ˚C until stabilization (approximately 10 d) after the rainfall simulation experiments are completed and the mass of the empty box from the total mass.

The total precipitation volume (VP_{TOT}) is calculated by closing the water mass balance as follows:

$$VP_{TOT} = VD_{TOT} + VR_{TOT} + \Delta S_{TOT} \quad (1)$$

The precipitation intensity PI(t) is set to (VP_{TOT} /T) for the duration of the rainfall simulation and 0 otherwise, assuming constant intensity. T is the rainfall duration.

If a tracer (e.g., bromide, deuterium oxide) is used, the event water fraction (i.e., fraction of flow from current rain event) can be calculated through a two end member mixing model. Assuming a known concentration c_s in the soil water prior to the experiment (e.g., $c_s = 0$ if no tracer has been added previously), a known concentration c_p in the tracer-enriched artificial rainwater, and a measured drainage concentration C_D, we can decompose Q_D by applying the water mass conservation hypothesis:

$$Q_D = Q_{Dev} + Q_{Dpre} \quad (2)$$

and the tracer mass conservation hypothesis:

$$Q_D \times c_D = Q_{Dev} \times c_p + Q_{Dpre} \times c_s \quad (3)$$

where $Q_{D\ ev}$ is the discharge of water from the current rain event in the drainage and $Q_{D\ pre}$ is the discharge of pre-event water in the drainage (water that was stored in the soil before the rain event). By substituting Equation 2 into Equation 3, we can then determine

$$Q_{Dev} = Q_D \times \frac{(c_D - c_s)}{(c_p - c_s)} \quad (4)$$

where $(c_D - c_s) / (c_p - c_s)$ represents the event water fraction f_{ev}.

The overland flow coefficient CR for a whole event (i.e., the period between the start of precipitation to end of outflow) and at a time t during the event CR(t) are calculated as cumulative overland flow volume (of the whole event or up to t, respectively) divided by the cumulative precipitation volume (of the whole event or up to t, respectively).

2.4 | Technical validation

2.4.1 | Homogeneity and stability of simulated precipitation

The spatial homogeneity of the simulated rainfall was experimentally validated by placing 105 cylindrical plastic containers with a diameter of 4 cm and a height of 5.8 cm inside the empty sampling case, aligning the plastic containers and the base frame at the top edge. Rain was then simulated for approximately 20 min and the water height in each container was measured. Temporal variability and overall intensity were verified by simulating rain on an empty sampling device and continuously measuring the discharge. We proceeded like this for various full cone sprinkler nozzles of the Lechler 490 series generating intensities ranging from 50 mm h^{-1} (490.488.30) to 100 mm h^{-1} (490.608.30).

2.4.2 | Contaminant transfer test

The device was tested on a colluvial brown calcareous pasture soil with silt-loam texture from Le Pradel, 07170 Mirabel in France (44.58206° N, 4.49998° E, WGS84). The site is part of the OHMCV observatory and is presented in Nord et al. (2017). Fresh cow dung (80% humidity, cows not treated with avermectins) was contaminated with IVM (veterinary oral solution ORAMEC) to a final concentration of 3 mg kg^{-1} fresh weight, corresponding to the highest observed concentration in dung after pour-on treatment (Herd et al., 1996). The contaminated cow dung was homogenized and shaped by hand into a circular cake, 20 cm in diameter. It was placed with its edges 30 cm from the downhill edge, 10 cm from the uphill edge and 5 cm from both sides of the sampling device (Supplemental Figure S5). Artificial rain (distilled water with 130 mg L^{-1} bromide tracer for the calculation of event water fractions) was applied for 1 h at an intensity of 92 mm h^{-1}, corresponding to a rainfall event with a return period of 10–20 yr for this region (Beuerle, 2021). The same intensity over half an hour corresponds to return period of about 5 yr. The length of the simulated rainfall event allows following the evolution of water and contaminant fluxes, while the event can still be used to approximate the water and contaminant transfer during a shorter more frequent event by analyzing the beginning of the event. The experiment was conducted on semi-dry soil ($\theta_0 = 22\%$). Sampling and measurement were stopped 4 h after the start of the simulated rainfall. In total we collected 14 drainage samples and 9 overland flow samples. For the drainage samples, the collection interval varied from 2.5 min at the beginning of the experiment over 6 min during most of the simulation to 2 h for the last sample. For overland flow, the collection interval was 6 min at the beginning of the simulation and 8 min at the end.

2.5 | Water sampling and chemical analysis

Samples were collected in glass bottles (Schott Duran 500 ml), which were washed using a professional washing machine (Miele professional G 7883) and then heated to 500 °C for 3 h (Nabertherm L 9/11/B170 oven) before use to ensure analytical level cleanliness. Immediately after collection, the bulk water samples were split for different analyzes. In this test, the following analyses were carried out: major anions, dissolved organic carbon (not presented) and IVM. The coefficient of variation and limit of quantification determined for the IVM analyzes were <5% and 1 ng L^{-1}, respectively. More details on the chemical analysis, which is specific to our test experiment, can be found in the Supplemental Material file.

3 | RESULTS AND DISCUSSION OF THE TECHNICAL VALIDATION

3.1 | Rainfall simulation

3.1.1 | Homogeneity and stability

Here we present results obtained with the Lechler 490.680.30 sprinkler nozzle mounted 67 cm above the soil surface (center), which is the configuration used in the presented test. The coefficient of variation of rain intensity was 8% over the 78 spatially distributed samples that were not covered by the

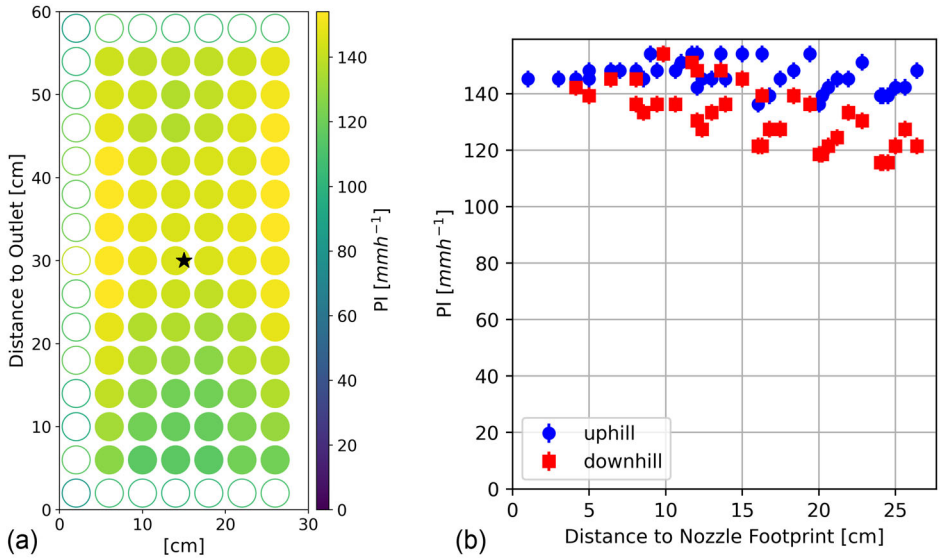

FIGURE 2 Validation of spatial homogeneity of rainfall. (a) Spatial distribution of rainfall intensity across the box given in color gradients and plotted at cm-coordinates of the box; $y = 0$ represents the outlet (bottom side of the box). The black star indicates the nozzle location. Empty markers represent containers partially covered by the border and not considered in the data analysis. (b) Rain intensity measured in plastic containers as a function of box-surface parallel distance to the nozzle footprint. Blue circles represent the locations uphill and red squares the locations downhill of the nozzle footprint. Error bars indicate the uncertainty of the water height measurement

border. The spatial distribution is shown in Figure 2. As expected, the 8° slope resulted in a slight decrease in intensity toward the bottom of the slope, where raindrop trajectory and dispersion are highest. Regarding temporal stability, the system produced small periodic variations in rain intensity of 10% with a period of 2.5–3 min due to pumping cycles with a constant average throughout the artificial rain event. With the Lechler 490.488.30 sprinkler nozzle, the coefficient of variation in rain intensity was 7% over the spatially distributed samples and the periodic variations due to pumping cycles were 10% with a period of 3–3.5 min.

3.1.2 | Limitations of the rainfall simulation protocol

The two sprinkler nozzles used Lechler 490.488.30 and 490.680.30 generate fine droplets (mean diameter $[D_m] = 0.69$ and 0.75 mm, respectively) with low kinetic energy ($E_{kin} = 1.48$ J m^{-2} mm^{-1} and 2.76 J m^{-2} mm^{-1}, respectively). For comparison, we analyzed disdrometric rainfall data from the nearby La Souche meteorological station from July 2012 to March 2020 (OHMCV, 2012). For rainfall intensities between 50 and 100 mm h^{-1}, the average D_m was 1.05 mm (0.41–1.94) and the average E_{kin} was 63.4 J m^{-2} mm^{-1} (16.1–208.7). This shows that the simulated rain has less kinetic energy and slightly smaller drops than the observed average for similar precipitation intensities. While D_m is within the range of observed values, the kinetic energy is much lower. The size distributions of simulated raindrops measured with an *OTT Parsivel2* disdrometer are illustrated in Supplemental Figure S6.

The choice to generate fine droplets with low kinetic energy was made with the intention of preserving soil structure over several rainfall simulation experiments so that transfer through initially wet vs. dry soil could be compared for the same state of the soil surface. The soil surface itself being formed by natural precipitation and other processes in the field, which a rainfall simulator could most likely not perfectly imitate. Furthermore, the goal was to assess contaminant transfer in the dissolved phase rather than to study soil erosion processes. This has the drawback of not generating realistic erosion thus underestimating transfer of soil particles and sorbed contaminants. If this were the focus, a different nozzle could be used and mounted at higher distance from the soil surface to higher kinetic energy and larger drop size, as for example in Humphry et al. (2002).

Monitoring water discharge via the outflow mass has the advantage of being non-contact and independent of the receiver, which facilitates analytical level cleanliness and avoids stagnating zones that could trap water and sediment. It allows relatively precise measurement (depending on the scale's precision) and simple automated processing. However, it requires a particular rigor when changing the sampling containers. Assuming an average mass uncertainty of 2 g at each container change, we obtain a cumulated uncertainty of 30 ml (0.17 mm) over the whole event, which represents 0.2% of the total rainfall (92 mm).

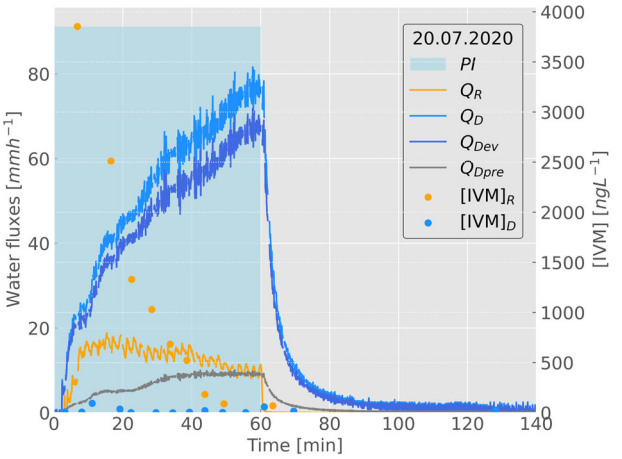

FIGURE 3 Dots represent ivermectin concentration ([IVM]) in drainage (blue, subscript D) and overland flow (orange, subscript R) during the rainfall simulation experiment, lines represent corresponding water discharges (same color). The drainage discharge is divided into event water (dark blue) and pre-event water (gray) using the bromide tracer concentrations. For illustration purposes, a sliding average of 15 triangularly weighted values is applied to the water discharges to smooth them

The calculation of soil water content by subtracting dry mass assumes that there is no significant change in soil dry mass during the experiments. For solid matter fluxes with water, this can be verified and corrected by drying or filtering the outflows and determining their dry mass. For plant growth and organic matter decomposition, this is considered negligible over a few days. For longer experiments, this adds uncertainty to the absolute water content. The evolution of water content and the magnitude of water content change (ΔS_{TOT}) are not affected. The uncertainty of weighing the entire soil box was 100 g, which corresponds to an uncertainty in the absolute volumetric water content of 2.8% (0.56 mm). It should be kept in mind that in the current setup (seepage face as lower boundary condition), the device is designed to study infiltration excess overland flow and leaching.

3.2 | Application of the experimental device to transfer of IVM

3.2.1 | Water and IVM fluxes

The event CR for the contaminant transfer test experiment was 13.5%, while $Q_R(t)$ is slightly decreasing over the course of the event (from 17 mm h^{-1} after 15 min to 10 mm h^{-1} after 60 min; Figure 3). The $Q_D(t)$ increases throughout the event reaching 75 mm h^{-1} after 60 min. The event water fraction in the drainage was relatively constant throughout the experiment (87%). The IVM concentration values are generally higher (69–3,854 ng L^{-1}) in overland flow with highest values in the beginning of the event and decreasing with time, while they are lower (0.5–94 ng L^{-1}) and much more irregular with multiple peaks in drainage. Overall, during the event, 174 ng IVM (0.058‰ of applied quantity) were exported via drainage, while 2,974 ng (0.99‰) were exported via overland flow. As this experiment was deployed to test the device, potential environmental implications are not discussed in this article and will be part of another study.

3.2.2 | Applicability of the experimental setup

The test confirmed the design of the box in terms of the feasibility of intact soil sampling and the overall setup for contaminant transfer experiments. The setup allows experiments to be conducted under controlled conditions (rain duration and intensity, initial soil condition, temperature, contaminant input) on intact field soil at a scale that preserves soil structure and especially macropores acting as preferential flow paths (drying cracks, earthworm galleries, root channels). Using the box for both sampling and rainfall experiments without the need to transfer the soil facilitates handling and increases experimental reliability. All mass balance components can be measured or calculated and water discharges as well as contaminant and tracer concentrations can be measured at very high (seconds) and high (minutes) intra-event frequency, respectively. Working with intact soils potentially limits the reproducibility of results due to sample heterogeneity and the large number of influencing factors, but nonetheless represents a more realistic approach to mimic real environmental systems and parameters. This is crucial for a better estimation of environmental risks by a more accurate, although less precise, prediction of environmental concentration.

This protocol can be adapted to different scientific questions. A wide range of rain intensities and durations can be selected by using different nozzles. The rain simulator could also be adapted to produce larger drops with higher kinetic energy if erosion is to be studied.

The presented device has the potential to contribute to a more realistic estimation of the transfer of environmental contaminants through and over the topsoil and thereby improve the environmental concentrations predicted in environmental risk assessments. Further application of this device is underway and we are open to collaborations willing to use it.

ACKNOWLEDGMENTS

We acknowledge the work of many engineers at the Institut des Géosciences de l'Environnement (IGE) of Grenoble for the construction of the devices (Service Technique) and for the chemical analysis (Plateau Air-O-Sol, with the funding of some of the equipment by the Labex OSUG@2020 - ANR10 LABX56). Bernard Mercier (IGE) is thanked for having developed a program for serial communication with the

scales. Christine Baduel (IGE) is thanked for her expertise in setting up the SPE protocol at IGE. Céline Voiron (IGE) is thanked for her analytical support. The Domaine Olivier de Serres (Ardèche, France) is thanked for giving access to the study site and allowing soil sampling. The HyDRIMZ team is thanked for many fruitful discussions. The OHMCV SNO observatory of the INSU of CNRS is part of OZCAR Research infrastructure (https://www.ozcar-ri.org) that is supported by the French Ministry of Research Institutions and Universities.

AUTHOR CONTRIBUTIONS

Nico Hachgenei: Conceptualization, data curation, formal analysis, investigation, methodology, project administration, software, supervision, validation, visualization, writing - original draft. Guillaume Nord: Conceptualization, funding acquisition, investigation, methodology, resources, supervision, writing - review & editing. Lorenzo Spadini: Conceptualization, investigation, methodology, resources, supervision, writing - review & editing. Henri Mora: Investigation, methodology, resources. François Courvoisier: Formal analysis, investigation, software. Jean-François Sutra: Formal analysis, investigation. Jean-Pierre Vandervaere: Conceptualization, methodology, resources, writing - review & editing. Cédric Legoût: Conceptualization, writing - review & editing. Marie-Christine Morel: Conceptualization, validation, writing - review & editing. Jean Martins: Conceptualization, writing - review & editing. Anne Lespine: Data curation, writing - review & editing. Céline Duwig: Conceptualization, funding acquisition, investigation, methodology, resources, supervision, writing - review & editing.

CONFLICT OF INTEREST

The authors declare no conflict of interest.

ORCID

Nico Hachgenei https://orcid.org/0000-0002-0490-2103
Guillaume Nord https://orcid.org/0000-0001-5541-9368
Jean-Pierre Vandervaere https://orcid.org/0000-0002-9620-0589
Jean Martins https://orcid.org/0000-0003-0314-1311
Anne Lespine https://orcid.org/0000-0001-8153-8555
Celine Duwig https://orcid.org/0000-0003-1505-8996

REFERENCES

Archundia, D., Duwig, C., Spadini, L., Morel, M. C., Prado, B., Perez, M. P., Orsag, V., & Martins, J. M. F. (2019). Assessment of the sulfamethoxazole mobility in natural soils and of the risk of contamination of water resources at the catchment scale. *Environment International*, *130*(February), 104905. https://doi.org/10.1016/j.envint.2019.104905

Bachmair, S., Weiler, M., & Nützmann, G. (2009). Controls of land use and soil structure on water movement: Lessons for pollutant transfer through the unsaturated zone. *Journal of Hydrology*, *369*(3–4), 241–252. https://doi.org/10.1016/j.jhydrol.2009.02.031

Benecke, P., Beese, F., & van der Ploeg, R. R. (1976). Bodenhydrologische Methoden zur Untersuchung ungestörter, skelettreicher Böden. *Zeitschrift Für Pflanzenernährung Und Bodenkunde*, *139*(3), 361–371. https://doi.org/10.1002/jpln.19761390311

Beuerle, A. (2021). *Implémentation d'un modèle conceptuel distribué pour simuler l'effet de la variabilité spatiale de la pluie sur les transferts de surface*. ENSE3, G-INP Université Grenoble Alpes.

Bicudo, J. R., & Goyal, S. M. (2003). Pathogens and manure management systems: A review. *Environmental Technology (United Kingdom)*, *24*(1), 115–130. https://doi.org/10.1080/09593303093 85542

Boxall, A. B. A. (2017). Contamination from the agricultural use of growth promoters and medicines. In *Encyclopedia of the Anthropocene* (Volume 5, pp. 257–262). Elsevier Inc. https://doi.org/10.1016/B978-0-12-809665-9.09900-6

Boyle, M., Frankenberger, W. T., & Stolzy, L. H. (1989). The influence of organic matter on soil aggregation and water infiltration. *Journal of Production Agriculture*, *2*(4), 290–299. https://doi.org/10.2134/jpa1989.0290

Buchter, B., Leuenberger, J., Wierenga, P. J., & Richard, F. (1984). Preparation of large core samples from stony soils. *Soil Science Society of America Journal*, *48*(6), 1460–1462. https://doi.org/10.2136/sssaj1984.03615995004800060053x

Carmi, G., & Berliner, P. (2008). The effect of soil crust on the generation of runoff on small plots in an arid environment. *Catena*, *74*(1), 37–42. https://doi.org/10.1016/j.catena.2008.02.002

Chen, J., Yang, L., Chen, X., Ripp, S., Radosevich, M., & Zhuang, J. (2021). Bacterial mobility facilitated by soil depth and intact structure. *Soil and Tillage Research*, *209*, 104911. https://doi.org/10.1016/j.still.2020.104911

Darboux, F., Davy, P., Gascuel-Odoux, C., & Huang, C. (2002). Evolution of soil surface roughness and flowpath connectivity in overland flow experiments. *Catena*, *46*(2–3), 125–139. https://doi.org/10.1016/S0341-8162(01)00162-X

Duwig, C., Prado, B., Tinet, A.-J., Delmas, P., Dal Ferro, N., Vandervaere, J. P., Denis, H., Charrier, P., Gastelum Strozzi, A., & Morari, F. (2019). Impacts of land use on hydrodynamic properties and pore architecture of volcanic soils from the Mexican Highlands. *Soil Research*, *57*(6), 629. https://doi.org/10.1071/SR18271

Fernández, C., Porcel, M. A., Alonso, A., Andrés, M. S., & Tarazona, J. V. (2011). Semifield assessment of the runoff potential and environmental risk of the parasiticide drug ivermectin under Mediterranean conditions. *Environmental Science and Pollution Research*, *18*(7), 1194–1201. https://doi.org/10.1007/s11356-011-0474-8

Feyereisen, G. W., & Folmar, G. J. (2009). Development of a laboratory-scale lysimeter system to simultaneously study runoff and leaching dynamics. *Transactions of the ASABE*, *52*(5), 1585–1591.

Flury, M., Flühler, H., Jury, W. A., & Leuenberger, J. (1994). Susceptibility of soils to preferential flow of water: A field study. *Water Resources Research*, *30*(7), 1945–1954. https://doi.org/10.1029/94WR00871

Franzluebbers, A. (2002). Water infiltration and soil structure related to organic matter and its stratification with depth. *Soil and Tillage Research*, *66*(2), 197–205. https://doi.org/10.1016/S0167-1987(02)00027-2

Goss, M. J., Ehlers, W., & Unc, A. (2010). The role of lysimeters in the development of our understanding of processes in the vadose zone relevant to contamination of groundwater aquifers. *Physics and Chemistry of the Earth*, *35*(15–18), 913–926. https://doi.org/10.1016/j.pce.2010.06.004

Govers, G., Takken, I., & Helming, K. (2000). Soil roughness and overland flow. *Agronomie*, *20*(2), 131–146. https://doi.org/10.1051/agro:2000114

Guo, M., & Chorover, J. (2006). Leachate migration from spent mushroom substrate through intact and repacked subsurface soil columns. *Waste Management*, *26*(2), 133–140. https://doi.org/10.1016/j.wasman.2004.12.024

Hairsine, P., Moran, C., & Rose, C. (1992). Recent developments regarding the influence of soil surface characteristics on overland flow and erosion. *Soil Research*, *30*(3), 249. https://doi.org/10.1071/SR9920249

Hedlund, J., Longo, S. B., & York, R. (2020). Agriculture, Pesticide Use, and Economic Development: A Global Examination (1990–2014). *Rural Sociology*, *85*(2), 519–544. https://doi.org/10.1111/ruso.12303

Herd, R. P., Sams, R. A., & Ashcraft, S. M. (1996). Persistence of ivermectin in plasma and faeces following treatment of cows with ivermectin sustained-release, pour-on or injectable formulations. *International Journal for Parasitology*, *26*(10), 1087–1093. https://doi.org/10.1016/S0020-7519(96)80007-5

Humphry, J. B., Daniel, T. C., Edwards, D. R., & Sharpley, A. N. (2002). A portable rainfall simulator for plot – Scale runoff studies. *Applied Engineering in Agriculture*, *18*, 199–204. https://doi.org/10.13031/2013.7789

Kay, P., Blackwell, P. A., & Boxall, A. B. A. (2005a). A lysimeter experiment to investigate the leaching of veterinary antibiotics through a clay soil and comparison with field data. *Environmental Pollution*, *134*(2), 333–341. https://doi.org/10.1016/j.envpol.2004.07.021

Kay, P., Blackwell, P. A., & Boxall, A. B. A. (2005b). Column studies to investigate the fate of veterinary antibiotics in clay soils following slurry application to agricultural land. *Chemosphere*, *60*(4), 497–507. https://doi.org/10.1016/j.chemosphere.2005.01.028

Krogmann, H. (1986). Ungestörte Bodensäulen: Eine Methode zur Herstellung, Beregnung und Installation im Labor. *Zeitschrift Für Pflanzenernährung Und Bodenkunde*, *149*(3), 271–276. https://doi.org/10.1002/jpln.19861490304

Liebig, M., Fernandez, Á. A., Blübaum-Gronau, E., Boxall, A., Brinke, M., Carbonell, G., Egeler, H., Fenner, K., Fernandez, C., Fink, G., Garric, J., Halling-Sørensen, B., Knacker, T., Krogh, K. A., Küster, A., Löffler D., Cots, M. Á. P., Pope, L., Prasse, C., …, Duisy, K. (2010). Environmental risk assessment of ivermectin: A case study. *Integrated Environmental Assessment and Management*, *6*(SUPPL. (1),), 567–587. https://doi.org/10.1002/ieam.96

Martín M. Á., Martínez F. S. J., Perfect E., Lado M., Pachepsky Y. (2017) Soil structure and function in a changing world: Characterization and scaling. *Geoderma*, *287*, 1–3. https://doi.org/10.1016/j.geoderma.2016.08.015

Milleret, R., Le Bayon, R. C., Lamy, F., Gobat, J. M., & Boivin, P. (2009). Impact of roots, mycorrhizas and earthworms on soil physical properties as assessed by shrinkage analysis. *Journal of Hydrology*, *373*(3–4), 499–507. https://doi.org/10.1016/j.jhydrol.2009.05.013

Nizzetto, L., Futter, M., & Langaas, S. (2016). Are agricultural soils dumps for microplastics of urban origin? *Environmental Science and Technology*, *50*(20), 10777–10779. https://doi.org/10.1021/acs.est.6b04140

Nord, G., Boudevillain, B., Berne, A., Branger, F., Braud, I., Dramais, G., Gérard, S., Le Coz, J., Legoût, C., Molinié, G., Van Baelen, J., Vandervaere, J. P., Andrieu, J., Aubert, C., Calianno, M., Delrieu, G., Grazioli, J., Hachani, S., Horner, I., …, Wijbrans, A. (2017). A high space-time resolution dataset linking meteorological forcing and hydro-sedimentary response in a mesoscale Mediterranean catchment (Auzon) of the Ardèche region, France. *Earth System Science Data*, *9*(1), 221–249. https://doi.org/10.5194/essd-9-221-2017

Obimakinde, S., Fatoki, O., Opeolu, B., & Olatunji, O. (2017). Veterinary pharmaceuticals in aqueous systems and associated effects: An update. *Environmental Science and Pollution Research*, *24*(4), 3274–3297. https://doi.org/10.1007/s11356-016-7757-z

Observatoire Hydro-météorologique Méditerranéen Cévennes-Vivarais (OHMCV). (2012). *DSD network, La Souche*. Centre national de la recherche scientifique, Observatoire des sciences de l'Univers de Grenoble, Observatoire de Recherche Méditerranéen de l'Environnement. https://doi.org/10.17178/OHMCV.DSD.SOU.12-16.1

Popova, I. E., Bair, D. A., Tate, K. W., & Parikh, S. J. (2013). Sorption, leaching, and surface runoff of beef cattle veterinary pharmaceuticals under simulated irrigated pasture conditions. *Journal of Environmental Quality*, *42*(4), 1167–1175. https://doi.org/10.2134/jeq2013.01.0012

Rath, S., Pereira, L. A., Bosco, S. M. D., Maniero, M. G., Fostier, A. H., & Guimarães, J. R. (2016). Fate of ivermectin in the terrestrial and aquatic environment: Mobility, degradation, and toxicity towards *Daphnia similis*. *Environmental Science and Pollution Research*, *23*(6), 5654–5666. https://doi.org/10.1007/s11356-015-5787-6

Sadeghi, A. M., Isensee, A. R., & Shirmohammadi, A. (2000). Influence of soil texture and tillage on herbicide transport. *Chemosphere*, *41*(9), 1327–1332. https://doi.org/10.1016/S0045-6535(00)00028-X

Sarmah, A. K., Meyer, M. T., & Boxall, A. B. A. (2006). A global perspective on the use, sales, exposure pathways, occurrence, fate and effects of veterinary antibiotics (VAs) in the environment. *Chemosphere*, *65*(5), 725–759. https://doi.org/10.1016/j.chemosphere.2006.03.026

Schäfer, R. B., Caquet, T., Siimes, K., Mueller, R., Lagadic, L., & Liess, M. (2007). Effects of pesticides on community structure and ecosystem functions in agricultural streams of three biogeographical regions in Europe. *Science of the Total Environment*, *382*(2–3), 272–285. https://doi.org/10.1016/j.scitotenv.2007.04.040

Stuer-Lauridsen, F., Birkved, M., Hansen, L. P., Holten Lützhøft, H. C., & Halling-Sørensen, B. (2000). Environmental risk assessment of human pharmaceuticals in Denmark after normal therapeutic use. *Chemosphere*, *40*(7), 783–793. https://doi.org/10.1016/S0045-6535(99)00453-1

Williams, M. R., Coronel, O., McAfee, S. J., & Sanders, L. L. (2020). Preferential flow of surface-applied solutes: Effect of lysimeter design and initial soil water content. *Vadose Zone Journal*, *19*(1), 1–15. https://doi.org/10.1002/vzj2.20052

SUPPORTING INFORMATION

Additional supporting information may be found in the online version of the article at the publisher's website.

How to cite this article: Hachgenei, N., Nord, G., Spadini, L., Mora, H., Courvoisier, F., Sutra, J.-F., Vandervaere, J.-P., Legoût, C., Morel, M.-C., Martins, J., Lespine, A., & Duwig, C. (2022). A device to simulate contaminant transfer and surface and subsurface flow through intact soil monoliths. *Vadose Zone Journal*, *21*, e20184. https://doi.org/10.1002/vzj2.20184